



**HAL**  
open science

## 3D structure of three jumbo phage heads

Emmanuelle Neumann, Takeru Kawasaki, Grégory Effantin, Leandro Estrozi,  
Orawan Chatchawankanphanich, Takashi Yamada, Guy Schoehn

► **To cite this version:**

Emmanuelle Neumann, Takeru Kawasaki, Grégory Effantin, Leandro Estrozi, Orawan Chatchawankanphanich, et al.. 3D structure of three jumbo phage heads. *Journal of General Virology*, 2020, 10.1099/jgv.0.001487 . hal-02972759

**HAL Id: hal-02972759**

**<https://hal.univ-grenoble-alpes.fr/hal-02972759>**

Submitted on 30 Nov 2020

**HAL** is a multi-disciplinary open access archive for the deposit and dissemination of scientific research documents, whether they are published or not. The documents may come from teaching and research institutions in France or abroad, or from public or private research centers.

L'archive ouverte pluridisciplinaire **HAL**, est destinée au dépôt et à la diffusion de documents scientifiques de niveau recherche, publiés ou non, émanant des établissements d'enseignement et de recherche français ou étrangers, des laboratoires publics ou privés.

1 **3D structure of three jumbo phage heads**

2 Emmanuelle Neumann<sup>1</sup>, Takeru Kawasaki<sup>2</sup>, Grégory Effantin<sup>1</sup>, Leandro F. Estrozi<sup>1</sup>, Orawan  
3 Chatchawankanphanich<sup>3</sup>, Takashi Yamada<sup>2,4,\*</sup>, Guy Schoehn<sup>1,\*</sup>

4

5<sup>1</sup>Université Grenoble Alpes, CNRS, CEA, Institute for Structural Biology (IBS), F-38000,  
6Grenoble, France.

7<sup>2</sup> Department of Molecular Biotechnology, Graduate School of Advanced Sciences of Matter,  
8Hiroshima University, Higashi-Hiroshima 739-8530, Japan.

9<sup>3</sup> Plant Research Laboratory, National Center for Genetic Engineering and Biotechnology,  
10NSTDA, Pathum Thani, Thailand

11<sup>4</sup> Hiroshima Study Center, The Open University of Japan, Hiroshima 730-0053, Japan

12

13Emmanuelle Neumann : 0000-0003-4100-5054

14Takeru Kawasaki : 0000-0001-6581-8573

15Grégory Effantin : 0000-0002-6957-0875

16Leandro Estrozi : 0000-0003-2548-2547

17Orawan Chatchawankanphanich : 0000-0003-4676-7904

18Takashi Yamada : 0000-0002-3225-4182

19Guy Schoehn : 0000-0002-1459-3201

20

21

22\*Corresponding authors:

23**Dr Guy Schoehn. Tel: 00-33-4-57-42-85-68**

24**Email: [guy.schoehn@ibs.fr](mailto:guy.schoehn@ibs.fr)**

25Dr Takashi Yamada Tel: 00-81-82-424-7752

26Email : [tayamad@hiroshima-u.ac.jp](mailto:tayamad@hiroshima-u.ac.jp)

27

28

29Running title: **3D structure of three jumbo phage heads**

30

31Keywords : jumbo phage, structure, head, electron microscopy

32

33

## 34ABSTRACT

35Jumbo phages are bacteriophages that carry more than 200 kbp of DNA. In this study we  
36characterized two jumbo phages ( $\Phi$ RSL2 and  $\Phi$ XacN1) and one semi-jumbo phage ( $\Phi$ RP13)  
37at the structural level by cryo-electron microscopy. Focusing on their capsids, three-  
38dimensional structures of the heads at resolutions ranging from 16 Å to 9 Å were calculated.  
39Based on these structures we determined the geometrical basis on which the icosahedral  
40capsids of these phages are constructed, which includes the accessory and decorative proteins  
41that complement them. A triangulation number novel to *Myoviridae* ( $\Phi$ RSL2; T=21) was  
42discovered as well as two others which are more common for jumbo phages (T=27 and  
43T=28). Based on one of the structures we also provide evidence that accessory or decorative  
44proteins are not a prerequisite for maintaining the structural integrity of very large capsids.

45

46

## 47Introduction

48Bacteriophages are viruses that infect bacteria. They are extremely numerous and the number  
49of known bacteriophages has increased at a rate of approximately 100 per year for decades  
50[1]. An increasing number of studies have suggested that bacteriophages are an attractive  
51option for alternatives to antibiotics [2]. Bacteriophages can be polyhedral, filamentous, or  
52pleomorphic and may have either a long, short, contractile, or flexible tail. Some are even tail-  
53less. They can contain either single- or double-stranded DNA or RNA. Caudal bacteriophages  
54represent the vast majority of known bacterial viruses and have been classified in different  
55families according to their tail morphology which include *Siphoviridae* (long flexible tail),  
56*Myoviridae* (long contractile tail), and *Podoviridae* (short tail). Bacteriophages carrying more  
57than 200 kbp of DNA are commonly known as “jumbo phages” [3, 4].

58

59The capsids of phages have icosahedral symmetry and are constructed from a basic brick  
60which, until now, has always been based on the canonical structure of the HK97 major capsid  
61protein. The number of currently known jumbo phages is around 100 [5] with the dimension  
62of these phages varying from 100 to 160 nm in diameter for the head and a triangulation  
63number between 19 and 52 [6]. Only a few of the known jumbo phages have been  
64characterized structurally, including  $\Phi$ kZ [7],  $\Phi$ RSL1 [8],  $\Phi$ M12 [9] and  $\Phi$ N3,  $\Phi$ Pau,  
65 $\Phi$ PBS1,  $\Phi$ 121Q, and  $\Phi$ G [6]. The highest resolution of their three-dimensional structures has  
66been limited to 9 Å. Particularly within the jumbo phage family and more generally in the  
67bacteriophage world, viruses use different types of accessory or decorating proteins. Because  
68of the large size of their genome, they also exhibit large heads with high triangulation  
69numbers (usually higher than 20). The larger the genome is, the larger the capsid has to be.  
70This is a general rule in the virus world with a correlation between genome length and capsid  
71size[10]. However there are deviation to the rule: for the characterized jumbo phages, the  
72average density of packed DNA has been measured experimentally to be between 0.39 and  
730.55 bp/nm<sup>3</sup> which represent a variation of 40% [6].

74

75Towards the aim of contributing to a better understanding of the structural characteristics of  
76jumbo phages including DNA packing, we examined the structures of two large jumbo phages  
77( $\Phi$ RSL2 with a medium-sized genome of 224 kbp [11] and  $\Phi$ XacN1 with a large genome of  
78385 kbp [12]) and one smaller semi-jumbo phage ( $\Phi$ RP13) carrying also a smaller genome of  
79about 180 kbp (phages with a genome smaller than 200 kbp but close to 200 kbp are defined  
80as semi-jumbo phages). Here we present three new three-dimensional structures of jumbo

81phage heads: two of them representing new examples of known triangulation numbers (T=27  
82and T=28) and one new type of geometry (T=21) never described for a *Caudovirales*. Two of  
83phage heads are decorated with different proteins (on the outside and also on the inside of the  
84capsid) but  $\Phi$ XacN1 appears to be naked, with the capsid built only by one type of protein  
85(with the exception of the vertices). The DNA packing density is in the common range of 0.39  
86and 0.55 bp/nm<sup>3</sup> for  $\Phi$ XacN1 and  $\Phi$ RP13 but much lower for  $\Phi$ RSL2 (0.29). All together  
87this is showing that there is no rule that can be applied for phages neither in the capsid  
88composition nor in the genome-capsid size correlation.

89

90

## 91Materials and Methods

### 92Bacteriophage production and purification

93Ralstonia phages  $\Phi$ RSL2 [11] and  $\Phi$ RP13 [13] were isolated from Japan and Thailand,  
94respectively. They were propagated with *Ralstonia solanacearum* MAFF 106603 as the host.  
95Host bacterial cells were cultured in CPG medium containing 0.1% (w/v) casamino acids,  
961.0% (w/v) peptone, and 0.5% (w/v) glucose [14] at 28°C with shaking at 200-300 rpm. When  
97the cultures reached an OD<sub>600</sub> of 0.05, each bacteriophage was added at a multiplicity of  
98infection (MOI) of 0.1. After culturing for a further 12-24 h, the cells were removed by  
99centrifugation at 5,000 x g for 15 min at 4°C in a R12A2 rotor in a Hitachi himac CR21E  
100centrifuge. The supernatant was membrane-filtered (0.45- $\mu$ m pore; Steradisc, Kurabo Co.  
101Ltd., Osaka, Japan), and the pellet was dissolved in SM buffer (50 mM Tris-HCl at pH 7.5,  
102100 mM NaCl, 10 mM MgSO<sub>4</sub>, and 0.01% gelatin) after centrifugation at 15,000 x g for 1h at  
1034°C. For further purification, the phage suspension was layered on a 20-60% sucrose gradient  
104and centrifuged with a P28S rotor in a Hitachi CP100 $\beta$  ultracentrifuge at 40,000 x g for 1 h.  
105The purified phages were stored at 4°C. Xanthomonas phage  $\Phi$ XacN1 [12] was isolated in  
106Japan and propagated with *Xanthomonas citri* MAFF 301080 as the host. *Xanthomonas* cells  
107were cultured in NB medium (Difco, BBLBD, Cockeysville, MD, USA) at 28°C with  
108shaking at 220 rpm. When cultures reached an OD<sub>600</sub> of 0.03,  $\Phi$ XacN1 was added at a MOI of  
1090.1. After culturing for a further 12-24 h, the cells were removed by centrifugation at 5,000 x  
110g for 15 min at 4°C and the supernatant was membrane-filtered as above.  $\Phi$ XacN1 was  
111pelleted by centrifugation at 15,000 x g for 1h at 4°C and dissolved in SM buffer as above.  
112For further purification, the phage suspension was layered on a 20-60% sucrose gradient and  
113centrifuged at 40,000 x g for 1 h as above.

114

115

#### 116 Negative staining electron microscopy

117 Negative-stain grids were prepared using the mica-carbon flotation technique [15]. Briefly,  
118 samples were adsorbed on the clean side of a carbon film previously evaporated on mica and  
119 then stained using 2% (w/v) Ammonium Molybdate pH 7.5 for 30 s. The sample/carbon  
120 ensemble is then transferred to a grid and air-dried. Images were acquired under low dose  
121 conditions ( $<30 \text{ e}^-/\text{\AA}^2$ ) on a Tecnai 12 FEI electron microscope operated at 120 kV using a  
122 Gatan ORIUS SC1000 camera (Gatan, Inc., Pleasanton, CA).

123

#### 124 Cryo-EM

125 3.5  $\mu\text{l}$  of concentrated sample were applied to glow discharged (25 mA, 40 s) R3.5/1  
126 quantifoil copper grids (Quantifoil Micro Tools). The excess of solution was blotted using a  
127 Vitrobot (20°C, 100% humidity, 2-s blotting time, and blot force 1) and subsequently flash-  
128 frozen in liquid ethane.

129 The grids were transferred to a Tecnai F30 Polara electron microscope working at 300 kV.  
130 Movies (40 frames of 0.1 s and a dose of 1 electron/ $\text{\AA}^2$  per frame) were recorded manually on  
131 a K2 summit direct electron detector using the low dose module in the GMS3 software  
132 (Gatan) software at a nominal magnification of  $\times 12,000$  in super resolution mode (1.64  $\text{\AA}$  per  
133 pixel at the sample level for  $\Phi\text{RSL2}$ ) and  $\times 20,000$  in counting mode (1.94  $\text{\AA}$  per pixel at the  
134 sample level for  $\Phi\text{XacN1}$  and  $\Phi\text{RP13}$ ).

135

#### 136 Image Analyses

137 For the  $\Phi\text{RSL2}$  dataset, the re-alignment of the frames has been performed automatically  
138 using the Latitude S software. For the two other datasets, Motioncor2 has been used excluding  
139 frames 1 and 2 [16]. CTF parameters were determined using GCTF [17].

140

#### 141 $\Phi\text{RSL2}$

142 The images have been binned four times (final pixel size of 6.57  $\text{\AA}$ ). The initial 3D model of  
143 full  $\Phi\text{RSL2}$  capsids has been calculated with the RICO software [18]. Thereafter all image  
144 analyses and capsid reconstructions have been performed using the Relion software [19]  
145 imposing icosahedral symmetry. The final reconstruction includes 250 particles out of 499  
146 for a resolution of 16  $\text{\AA}$  (FSC determined using the gold-standard method implemented in  
147 Relion [19] at 0.143 threshold; Supplementary Figure 1).

#### 148 $\Phi\text{XacN1}$ and $\Phi\text{RP13}$

149The images have been binned two times (final pixel size of 3.88 Å). All the image analysis  
150including generation of an initial model have been performed using the Relion software [19].  
151The final reconstruction of ΦXacN1 and ΦRP13 respectively includes 1149 and 669 particles  
152for a resolution of 9.1 Å and 9.4 Å (FSC determined using the gold-standard method  
153implemented in Relion [19] at 0.143 threshold; Supplementary Figure 1).

154Reducing the binning to 2 for ΦRSL2 and no binning for ΦXacN1 and ΦRP13 did not  
155improve the resolution of the corresponding map.

156Figures were generated using Chimera [20]. All the statistics are summarized in Table 1.

157

158Fitting of the bacteriophage HK97 MCP into the EM map

159The X-rays structure of HK97 MCP (pdb 2FT1) was fitted into the ΦXacN1 and ΦRP13 map  
160using Chimera [20]. Briefly the entire structure (7 monomers) was first roughly placed by  
161hand in the EM map and in a second step only one monomer was used. For this second step,  
162the long alpha helix of HK97 monomer, which is easily recognizable was used as a landmark.  
163Final refinement of the fitting was performed using the Chimera function “fit in map”.

164

## 165Results

166Two of the bacteriophages described here (ΦRSL2 [11] and ΦRP13 [13]) were isolated from  
167the phytopathogen *Ralstonia solanacearum*. The third one (ΦXacN1 [12]) also a jumbo  
168phage, was isolated from the phytopathogen *Xanthomonas citri*. The three phages belong to  
169the *Caudovirales* order and exhibit the typical *Myoviridae* morphology with a contractile tail  
170and an isometric head (Figure 1). Negative staining images of ΦRSL2 (Figure 1A) clearly  
171show that the tail is decorated by fibres at two different levels (arrows). For ΦXacN1, an  
172annular structure of unknown function is present around the tail (Figure 1B, arrow). ΦRP13  
173differs from the other two phages because it exhibits a double-layered baseplate like the  
174Twort-like phage Φ812 [21]. The [tail length]:[capsid diameter] ratios are quite different  
175among the different viruses (Table 2). For this study we mainly focused our structural  
176analyses on the virus head.

177

### 178ΦRSL2

179Cryo-electron microscopy images show that the sample was a mixture between  
180bacteriophages with a head full of DNA and others which have released their DNA (appearing  
181as light shades in the images). Only capsids full of DNA were selected to perform icosahedral  
182image analysis. The resulting structure shows a capsid having a diameter of 139 nm from

183vertex to vertex (5-fold axis) and 128 nm along the 2-fold axis. The triangulation number,  
184which determines the number of protein copies forming the capsid, is  $T=27$  and was deduced  
185from the hexagonal lattice present on the surface. It was calculated using the formula  
186 $T=h^2+hk+k^2$  where  $h$  and  $k$  are the number of local symmetry axes to be crossed to go from  
187one 5-fold axis to the next [22]. For  $\Phi$ RSL2, the observed numbers were  $h=3$  and  $k=3$  (Figure  
1882A).

189

190The resolution obtained for  $\Phi$ RSL2 was limited to 16 Å due to a limited number of particles  
191(250 particles; Figure 2A and Table 1). Each facet of the capsid is flat and composed of 13  
192hexamers. These hexamers as well as the pentamers are most probably made of the same  
193protein: the major capsid protein (MCP) which, for this virus, is encoded by ORF117  
194(predicted size of 82,440 Da but observed size of 70 kDa according to SDS-PAGE and LC-  
195MS/MS analyses as described before [11]). This is the largest known MCP. An icosahedral  
196capsid with a triangulation number of  $T=27$  is assembled from 27x60 asymmetric units (or  
19720x13 hexamers plus 12 pentamers). In the case of a caudal bacteriophage, a pentamer must  
198be removed because one of the vertices is occupied by the portal. The total number of MCPs  
199in this capsid is therefore 1615 since it appears at this resolution that the 11 vertices that do  
200not bind the tail are composed of the same protein.

201

202A hollow tube can be found at the centre of each hexamer with a diameter of 40 Å and a  
203length of 70 Å. The 260 cylindrical structures project outward from the capsid and appear to  
204cross the capsid and slightly extend out from the inner face of the hexamer (Figure 3C). The  
205stoichiometry of this protein is difficult to assess at this resolution as it lacks recognisable  
206features. The outside of the capsid is further decorated with another cylindrical protein (70 Å  
207in length and 30 Å in diameter) that is bound to the periphery of the hexamers and lying  
208parallel to the capsid surface. It associates in 810 dimers and forms bridges between  
209neighbouring hexamers/pentamers (Figure 3B). The structure and organisation of the dimer is  
210reminiscent from that observed in the  $\Phi$ KZ [7] and  $\Phi$ PBS1 capsids [6] which have the same  
211triangulation number. It is interesting to note the presence of extra densities on the inside of  
212the capsid, at the level of the 5-fold axis (Figure 3A, black arrows). This kind of structure is  
213different from the one observed in  $\Phi$ RSL1 which exhibits a much more complex structure  
214made of a trimer and a dimer [8]. Isosurface visualisation of these densities from the inside of  
215the capsid (Figure 3D) shows that they are directly connected to the capsid at the 5-fold axis  
216level (central globular structures) but also to the base of the cylindrical structures present at

137

14



217the centres of each hexamer. The nature of these densities is unknown, but they may  
218correspond to proteins or DNA/protein complexes that link the DNA to the capsid and allow  
219the DNA to be organised.

220

221Focusing on the inside of the capsid, one can note the absence of DNA organised in  
222concentric layers which is probably not due to the lack of resolution as it becomes visible at  
223about a 20 Å resolution. It is possible to distinguish a hexagonal mono domain organisation of  
224DNA with a cylindrical rod spanning the interior of the head and oriented along the tail axis  
225(dotted rectangle at bottom of Figure 1A; Supplementary Figure 2C). When  $\Phi$ RSL2 was  
226exposed to a very high dose of electrons ( $>100 \text{ e}^-/\text{Å}^2$ ), an “inner body” similar to the one  
227observed for  $\Phi$ KZ [23] and  $\Phi$ 121Q [6] can be visualized. However, this bubblegram is  
228slightly different from that observed with  $\Phi$ KZ as it has an arch at one end of the cylinder that  
229is close to the tail. This arch is reminiscent of the structures visible under the 5-fold axis in  
230Figure 3D.

231

### 232 $\Phi$ XacN1

2331149 particles have been used out of 1775 to obtain a 9 Å resolution three-dimensional map  
234of the  $\Phi$ XacN1 head. Only particles loaded with DNA were analysed. The diameter of the  
235final reconstructed full capsid is 139.5 nm from vertex to vertex and 116 nm along the 2-fold  
236axis (Figures 1B and 2B). The triangulation number of this head is  $T=28$  ( $h=4, k=2$ ). The  
237major capsid protein of  $\Phi$ XacN1 is 463 aa in length and about 49 kDa in mass as described  
238before [12]. Even with the medium resolution of this reconstruction, it was possible, due to the  
239presence of a long “spinal” alpha helix, to unambiguously fit the X-ray structure of HK97  
240[24] into the cryo-electron microscopy map (Supplementary Figure 3A). The handedness of  
241the structure is therefore most likely to be *dextro* ( $T=28, d$ ). There are only two other known  
242capsids from the *Caudavirales* order where three-dimensional reconstructions show such  
243symmetry:  $\Phi$ 121Q [6] and PhAPEC6 [25].

244

245The structure of the external and internal faces of the capsid is very smooth compared to other  
246phages (Figures 2B, 3F, and 3G). This is especially true if compared with  $\Phi$ 121Q which  
247harbours two types of decoration proteins at the periphery and on the middle of the hexamer.  
248The only protruding components are located at the 5-fold axis with the presence of a turret-  
249like structure (dimensions of 38 Å in height and 60 Å in diameter; Figure 3F). This kind of  
250extension is quite common in the bacteriophage world [8, 9, 26]. Inspection of the central

251 slice of the three-dimensional reconstruction clearly shows that there are at least six  
252 concentric layers of DNA separated by 23.6 Å (Figure 3E). When irradiated at a high electron  
253 dose, the  $\Phi$ XacN1 head did not exhibit any bubblegram-type structure (data not shown).

254

### 255 $\Phi$ RP13

256 Image analysis of the  $\Phi$ RP13 head started with 1311 particles. The best 669 particles yielded  
257 a three-dimensional reconstruction image at 9 Å resolution. This capsid shows a triangulation  
258 number of  $T=21$ , which was the smallest triangulation (and dimensions) of the three jumbo  
259 phages analysed here. The diameter of the particle from vertex to vertex is only 114 nm and  
260 between two opposed two-fold axes it is 97 nm. The obtained resolution enabled fitting of the  
261 HK97 X-ray structure into the  $\Phi$ RP13 capsid reconstruction leading to the assumption that the  
262 capsid handedness is  $T=21$  *laevo* (supplementary Figure 3B). The  $\Phi$ RP13 phage is the first  
263 HK97-related phage to exhibit this kind of triangulation number. Only lipidic phages like  
264  $\Phi$ PM2 [27], FLiP (*Flavobacterium*-infecting, lipid-containing phage [28]), or P23-77 [29]  
265 have shown an organization with similar geometry but with a pseudo  $T=21$  *dextro*  
266 triangulation number. These types of phages do not use the canonical HK97 hexameric  
267 structure to build up their capsid but rather incorporate an adenovirus-like trimeric structure.  
268 Based on the three-dimensional structure it is clear that the vertices of the capsid are built by  
269 the same protein as the facet (Figures 3I and 3J, pentamer and hexamer). The capsid is  
270 therefore composed of 1255 copies of the major capsid protein (20x10 hexamers per facet  
271 plus 11 pentamers).

272

273 Decoration proteins can be found on the top of the major capsid protein in a position crossing  
274 local two-fold axes somewhat similar to what was observed in  $\Phi$ RSL2. The shape of the  
275 dimeric decoration proteins surrounding the hexamer is more globular in case of  $\Phi$ RSL2  
276 compared to that of  $\Phi$ RP13. The  $\Phi$ RP13 decoration protein also appears to be hollow. On the  
277 inside of the particle, in the middle of each hexamer, one can also find a globular extra density  
278 (Figure 3J, right, arrow). On the DNA level, it is possible to distinguish at least five  
279 concentric layers of DNA separated by 26.3 Å. Like  $\Phi$ XacN1, an irradiation-sensitive inner  
280 body was not detected for this virus (data not shown).

281

282

### 283 Discussion

284 We determined the icosahedral capsid structures of three jumbo phages. Two of these phages  
285 are representatives of known triangulation number groups ( $T=27$  and  $T=28$ ), whereas the third  
286 one has a triangulation symmetry number that was not previously known to exist for caudal  
287 bacteriophages ( $T=21,1$ ). Surprisingly,  $\Phi XacN1$  has a smaller size compared to  $\Phi RSL2$  even  
288 though it has a higher triangulation number, but this may be due to the difference in size of  
289 their respective MCPs (46 Da vs 70 kDa). The distance between the centre of two adjacent  
290 hexamers is slightly higher for  $\Phi RSL2$  compared to  $\Phi XacN1$  and  $\Phi RP13$  (120 Å vs 113 Å,  
291 respectively). Different decoration proteins have been visualized on the outer portion of  
292  $\Phi RSL2$  and within its inner area. In contrast,  $\Phi XacN1$  has the most basic capsid of the three  
293 phages studied here as no decoration proteins were observed on the exterior of the capsid.  
294 This proves that these accessory proteins are not essential to ensure the solidity of  
295 bacteriophage capsids, even when faced with the enormous internal pressures required to  
296 compact up to 400 kbp of DNA. For  $\Phi RSL2$ , because its MCP is much larger compared to the  
297 other two phages, one cannot be completely sure if the dimer present at the periphery of the  
298 hexamer is an extra protein or part of the MCP itself. However, it is likely that this dimer  
299 consists of accessory proteins since the same kind of dimer is present in  $\Phi KZ$  and  $\Phi PBS1$  and  
300 because the MCPs are much smaller in these phages. A new kind of phage decoration protein  
301 that forms a hollow tube was also found in the  $\Phi RSL2$  capsid. One would need to study this  
302 at higher resolution to determine what role this protein may have.

303

304  $\Phi RSL2$  carries only 224 kbp of DNA but it has the largest capsid.  $\Phi RSL2$  is also the only  
305 phage in this study that has an inner body that does not exhibit concentric organisation of  
306 DNA layers within its three-dimensional structure. According to the structure we determined,  
307 large protein extensions are present on the inner part of the capsid and the DNA appears to be  
308 connected to the lower part of the hollow tube present at the centre of each hexamer. All of  
309 this together suggests that there are different types of DNA organisation in the jumbo phage  
310 world: one organised around an inner body with DNA connected to the capsid through  
311 dedicated structures near the 5-fold axes of the capsid; and another one as classical toroidal  
312 structures.

313 Two out of the three phages exhibits a “classical” DNA packing density of 0.49 and 0.39  
314 whereas the third one has as very low one:  $\Phi RSL2$  (0.29). This shows that the exceptions still  
315 exist and also shows the value of continuing extensive structural studies on viruses.

316

317The  $\Phi$ RP13 capsid protects 180 kbp of DNA: less than most jumbo phages but more than  
318classical bacteriophages.  $\Phi$ N3 DNA is 207 kbp for T=19,1 and with a capsid diameter of 120  
319nm (vertex to vertex) compared to 114 nm for  $\Phi$ RP13 [6]. Because the capsid dimensions and  
320the DNA size are in the same range for  $\Phi$ N3 and  $\Phi$ RP13, and even if  $\Phi$ RP13 does not  
321technically meet the jumbo phage criteria ( $> 200$  kbp), one can say that  $\Phi$ RP13 belongs to a  
322new “semi-jumbo” category.

323

324

### 325**Conclusion**

326We found a new triangulation number symmetry to add to the bacteriophage morphology  
327catalogue as well as a new kind of decoration protein. Many triangulation numbers are  
328observed in nature.  $\Phi$ RP13 exhibits a higher T number than  $\Phi$ N3 but with DNA size that is  
329too small for jumbo phage classification. We propose that  $\Phi$ RP13 belongs to a new group of  
330semi-jumbo phages. It seems that the distinction between classical myophages and jumbo  
331phages is not clearly defined and that there is a continuum in the DNA sizes carried by  
332*Myoviridae*. The diversity of accessory/decoration proteins is enormous. One can imagine that  
333during evolution each phage has dipped into a common well to create its own combination of  
334decorative/accessory proteins. Extensive study of these accessory proteins would help to  
335discover novel protein properties (e.g. recognition of ligand).

336

337

338

### 339 **Data availability**

340Cryo-EM maps have been deposited in the Electron Microscopy Data Bank:

341 -  $\Phi$ RSL2 capsid map EMD 11178

342 -  $\Phi$ XacN1 capsid map EMD 11180

343 -  $\Phi$ RP13 capsid map EMD 11179

344Genome sequence accession numbers for the different bacteriophages are:

345

346 -  $\Phi$ RSL2 : AP014693

347 -  $\Phi$ XacN1 : AP018399

348 -  $\Phi$ RP13 : LC554890

349

### 350**Authorship Confirmation Statement**

351T.K. produced and purified the three bacteriophages. O.C. isolated  $\Phi$ RP13 in Thailand. G.S  
352and E.N. prepared cryo-EM grids. E.N. and G.S. collected cryo-EM data on a FEI Polara EM.  
353E.N. performed cryo-EM image processing and cryo-EM 3D reconstructions with the help of  
354GE and LFE. The manuscript was written by G.S., E.N. and T.Y. with input from all authors.  
355G.S. was responsible for the conception and direction of the work, analysing and interpreting  
356data and revising the final drafts of the manuscript. All co-authors have reviewed and  
357approved of the manuscript before submission and agree to be accountable for all aspects of  
358the work. This manuscript has been submitted solely to this journal and is not published, in  
359press, or submitted elsewhere.

360

### 361 **Acknowledgments**

362We thank Maria Bacia-Verloop for technical assistance; Aymeric Peuch for help with the  
363usage of the EM computing cluster.

364This work used the platforms of the Grenoble Instruct-ERIC centre (ISBG ; UMS 3518  
365CNRS-CEA-UGA-EMBL) within the Grenoble Partnership for Structural Biology (PSB),  
366supported by FRISBI (ANR-10-INBS-05-02) and GRAL, financed within the University  
367Grenoble Alpes graduate school (Ecoles Universitaires de Recherche) CBH-EUR-GS (ANR-  
36817-EURE-0003).The electron microscope facility is supported by the Auvergne-Rhône-Alpes  
369Region, the Fondation Recherche Medicale (FRM), the fonds FEDER and the GIS-  
370Infrastructures en Biologie Sante et Agronomie (IBISA).

371

### 372 **Conflicts of interest**

373The authors declare that there are no conflicts of interest.

374

375

### 376 **Funding information**

377This work received no specific grant from any funding agency

378

379

380 **Figures legend:**

381

382 **Figure 1: Electron microscopy of bacteriophages  $\Phi$ RSL2,  $\Phi$ XacN1 and  $\Phi$ RP13.**

383

384A -  $\Phi$ RSL2

385 Top : Negative staining image of  $\Phi$ RSL2. The black arrows indicate decoration of the phage  
386 tail with fibrillary structures.

387 Bottom: Cryo electron microscopy image of the jumbo phage. The inner electron-dense body  
388 is highlighted by a rectangle or an arrow. The white arrow indicates some free DNA released  
389 from the bacteriophage.

390

391B –  $\Phi$ XacN1

392 Top : Negative staining image of  $\Phi$ XacN1. The arrows highlight an annular density  
393 decorating the phage tail.

394 Bottom : Cryo electron microscopy image of the jumbo phage. The arrow points to the same  
395 structure as the one highlighted in negative staining.

396

397C –  $\Phi$ RP13

398 Top : Negative staining image of  $\Phi$ RP13. The double arrow highlights the presence of a  
399 double layered baseplate in the virus. The inset show the bacteriophage in a contracted state  
400 with the inner tube of the tail sticking out.

401 Bottom : Cryo-EM image of  $\Phi$ RP13. The double arrow points to the double baseplate.

402

403 The scale bar represents 100 nm.

404

405

406 **Figure 2: Three-dimensional reconstruction of the three jumbo phages obtained from**  
407 **cryo-EM images.**

408

409 Three-dimensional reconstruction of the three jumbo phages represented as isosurface on the  
410 top of the figure. One facet is highlighted by a black triangle. The structures are color coded  
411 according to the radius of the particle as indicated in D.

412

413A diagram showing the organization of the asymmetric units in one of the facet of the  
414icosahedron is drawn for each virus. The organization of the hexamers in this facet makes it  
415possible to determine the triangulation number that characterizes each of the bacteriophages.  
416The different decoration proteins are also shown. The scale bars represent 20 nm.

417

418A –  $\Phi$ RSL2. The bacteriophage head has a triangulation number  $T=27$  ( $h=3$ ;  $k=3$ ;  $T=h^2 + hk$   
419+  $k^2$ ).

420

421B -  $\Phi$ XacN1. The bacteriophage head has a triangulation number  $T=28$ , *dextro* ( $h=4$ ;  $k=2$  ;  
422 $T=h^2 + hk + k^2$ ).

423

424C -  $\Phi$ RP13. The bacteriophage head has a triangulation number  $T=21$ , *laevo* ( $h=4$ ;  $k=1$  ;  
425 $T=h^2 + hk + k^2$ ).

426

427D – Color code used in A-C to color the capsids according to their radius (in nm).

428

429**Figure 3 : Central section and decoration protein**

430

431 **$\Phi$ RSL2**

432A – Half of the central section of the  $\Phi$ RSL2 density map. The protein density is in white.  
433Black arrows are highlighting densities on the inner part of the capsid. The white asterisk is  
434highlighting the cylindrical spike and the white arrow the dimer around the hexamers. The  
435scale bar represents 20 nm.

436

437B - Schematic view (left) and enlarged isosurface view (center) of the 5-fold axis showing  
438that the vertex is surrounded by dimers. The vertex is also prominent compared to the rest of  
439the capsid.

440

441C - Schematic view (left) and enlarged isosurface view (center) of one pseudo 6-fold axis  
442showing that the hexamers are surrounded by dimers and that there is a hollow cylindrical  
443density sticking out from its center. On the right, isosurface view of a hexamer seen from the  
444inside of the capsid. The arrow is pointing to the inner part of the spike present in the center  
445of the hexamer.

446

447D - Detailed view of the inside of the capsid along the 5-fold axis. The blue densities are  
448corresponding to the extra densities indicated in A by the arrows. They represent probably  
449nucleoprotein complexes involved in the DNA organization.

450

#### 451 **$\Phi$ XacN1**

452E - Half of the central section of the PhXacn1 density map showing that the capsid is roughly  
453smooth. Turret-like structures are only seen at the 5-fold axes, and some extra densities are  
454also visible under the 5-fold axes (arrow). It is possible to distinguish at least 6 concentric  
455layers of DNA. The protein/DNA densities are in white. The scale bar represents 20 nm.

456

457F - Schematic view (left) and enlarged isosurface view (center) of the 5-fold axis showing the  
458vertex composition. The right panel is a side view of the vertex showing the extra protein  
459forming the turret-like structure.

460

461G - Schematic view (left) and enlarged isosurface view (center) of one pseudo 6-fold axis  
462showing that the capsid is quite smooth and probably only composed by the major capsid  
463protein.

464

#### 465 **$\Phi$ RP13**

466H - Half of the central section of the  $\Phi$ RP13 density map showing that the capsid is decorated  
467by dimers (black arrow). No extra-densities are visible neither on the outside nor on the inside  
468of the 5-fold axes. It is possible to distinguish at least 5 concentric layers of DNA. The  
469protein/DNA densities are in white. The scale bar represents 20 nm.

470

471I - Schematic view (left) and enlarged isosurface view (center) of the 5-fold axis showing that  
472the vertex is surrounded by dimers. The protein forming the vertex has, at this resolution, the  
473same shape as the one forming the hexamers (the major capsid protein) (see J).

474

475J - Schematic view (left) and enlarged isosurface view (center) of one pseudo 6-fold axis  
476showing that the hexamer formed by the MCPs is surrounded by dimers. The right panel is  
477showing an isosurface view of a hexamer seen from the inside of the capsid. The arrow is  
478pointing to an extra density which is probably a non-identified protein.

479

480



481**Table 1 : Electron microscopy statistics for the image analysis of the three**  
482**bacteriophages.**

483

484**Table 2 : Dimensions of the different parts of the three bacteriophages (capsid, tail and**  
485**DNA).** The inner volume of the capsid has been measured using UCSF Chimera as described  
486in [6].

487

488

489

490

491

492

493 References

494

4951 - Ackermann HW. 5500 Phages examined in the electron microscope. *Arch Virol.* 4962007;152(2):227–243. doi:10.1007/s00705-006-0849-1

4972 - Nikolich MP, Filippov AA. Bacteriophage Therapy: Developments and Directions.

498 *Antibiotics (Basel)*. 2020;9(3):E135. Published 2020 Mar 24. doi:10.3390/antibiotics9030135

499

5003 - Hendrix RW. Jumbo bacteriophages. *Curr Top Microbiol Immunol*. 2009;328:229-240.

501doi: 10.1007/978-3-540-68618-7\_7

502

5034 - Yuan Y, and Gao M, Jumbo bacteriophages:an overview. *Front Microbiol*. 2017;8:403.

504doi: 10.3389/fmicb.2017.00403

505

5065 - Saad AM, Soliman AM, Kawasaki T, et al. Systemic method to isolate large 507bacteriophages for use in biocontrol of a wide-range of pathogenic bacteria. *J Biosci Bioeng.*

5082019;127(1):73–78. doi:10.1016/j.jbiosc.2018.07.001

509

510 6 - Hua J, Huet A, Lopez CA, et al. Capsids and Genomes of Jumbo-Sized Bacteriophages 511Reveal the Evolutionary Reach of the HK97 Fold. *mBio*. 2017;8(5):e01579-17. . doi:10.1128/

512mBio.01579-17

513

5147 - Fokine A, Kostyuchenko VA, Efimov AV, et al. A three-dimensional cryo-electron 515microscopy structure of the bacteriophage  $\Phi$ KZ head. *J Mol Biol*. 2005;352(1):117–124.

516doi:10.1016/j.jmb.2005.07.018

517

5188 - Effantin G, Hamasaki R, Kawasaki T, et al. Cryo-electron microscopy three-dimensional 519structure of the jumbo phage  $\Phi$ RSL1 infecting the phytopathogen *Ralstonia solanacearum*.

520 *Structure*. 2013;21(2):298–305. doi:10.1016/j.str.2012.12.017

521

5229 - Stroupe ME, Brewer TE, Sousa DR, Jones KM. The structure of *Sinorhizobium meliloti* 523phage  $\Phi$ M12, which has a novel T=191 triangulation number and is the founder of a new

524group of T4-superfamily phages. *Virology*. 2014;450-451:205–212.

525doi:10.1016/j.virol.2013.11.019

526

52710 - Cui J, Schlub TE, Holmes EC. An allometric relationship between the genome length and  
528virion volume of viruses. *J. Virol.* 2014 ;88(11) :6403-6410.

529

53011 - Bhunchoth A, Blanc-Mathieu R, Mihara T, et al. Two asian jumbo phages,  $\phi$ RSL2 and  
531 $\phi$ RSF1, infect *Ralstonia solanacearum* and show common features of  $\phi$ KZ-related phages.  
532*Virology.* 2016;494:56–66. doi:10.1016/j.virol.2016.03.028

533

53412 - Yoshikawa G, Askora A, Blanc-Mathieu R, et al. *Xanthomonas citri* jumbo phage XacN1  
535exhibits a wide host range and high complement of tRNA genes. *Sci Rep.* 2018;8(1):4486.  
536doi:10.1038/s41598-018-22239-3

537

53813 - Bhunchoth A, Phironrit N, Leksomboon C, et al. Isolation and characterization of  
539bacteriophages that infect *Ralstonia solanacearum* in Thailand. *ISHS Acta Horticulturae* 1207  
5402018 ; V International Symposium on Tomato Diseases: Perspectives and Future Directions in  
541Tomato Protection. pp. 155-162 doi:10.17660/ActaHortic.2018.1207.20

542

54314 - Horita M, and Tsuchiya K. Causal agent of bacterial wilt disease *Ralstonia*  
544*solanacearum*. In: National Institute of Agriculture Sciences (Ed.), MAAF Microorganism  
545Genetic Resources Manual No.12. 2002 National Institute of Agricultural Sciences, Tsukuba,  
546Japan, pp. 5-8.

547

54815 - Valentine R, Shapiro B, and Stadtman E. *Biochemistry.* 1968;7, 2143-2152

549

55016 - Zheng SQ, Palovcak E, Armache JP, Verba KA, Cheng Y, Agard DA. MotionCor2:  
551anisotropic correction of beam-induced motion for improved cryo-electron microscopy. *Nat*  
552*Methods.* 2017;14(4):331–332. doi:10.1038/nmeth.4193

553

55417 - Zhang K. Gctf: Real-time CTF determination and correction. *J Struct Biol.*  
5552016;193(1):1–12. doi:10.1016/j.jsb.2015.11.003

556

55718 - Estrozi LF, Navaza J. Ab initio high-resolution single-particle 3D reconstructions: the  
558symmetry adapted functions way. *J Struct Biol.* 2010;172(3):253–260.  
559doi:10.1016/j.jsb.2010.06.023

560

56119 - Scheres SH. RELION: implementation of a Bayesian approach to cryo-EM structure  
562determination. *J Struct Biol.* 2012;180(3):519–530. doi:10.1016/j.jsb.2012.09.006

563

56420 - Pettersen EF, Goddard TD, Huang CC, et al. UCSF Chimera--a visualization system for  
565exploratory research and analysis. *J Comput Chem.* 2004;25(13):1605–1612.  
566doi:10.1002/jcc.20084

567

568 21 - Nováček J, Šiborová M, Benešík M, Pantůček R, Doškař J, Plevka P. Structure and  
569genome release of Twort-like Myoviridae phage with a double-layered baseplate. *Proc Natl*  
570*Acad Sci U S A.* 2016;113(33):9351–9356. doi:10.1073/pnas.1605883113

571

57222 - Caspar D. and Klug A. Physical principles in the construction of regular viruses. *Cold*  
573*Spring Harbor Symp. Quant. Biol.* 1962 27:1-24. doi: 10.1101/sqb.1962.027.001.005

574

575

57623 - Wu W, Thomas JA, Cheng N, Black LW, Steven AC. Bubblegrams reveal the inner body  
577of bacteriophage  $\phi$ KZ. *Science.* 2012;335(6065):182. doi:10.1126/science.1214120

578

57924 - Helgstrand C, Wikoff WR, Duda RL, Hendrix RW, Johnson JE, Liljas L. The refined  
580structure of a protein catenane: the HK97 bacteriophage capsid at 3.44 Å resolution. *J Mol*  
581*Biol.* 2003;334(5):885–899. doi:10.1016/j.jmb.2003.09.035

582

58325 - Wagemans J, Tsonos J, Holtappels D, Fortuna K, Hernalsteens JP, Greve H, Estrozi LF,  
584Bacia-Verloop M, Moriscot C, Noben JP, Schoehn G, Lavigne R. Structural Analysis of  
585Jumbo Coliphage phAPEC6. *Int J Mol Sci.* 2020;21(9):E3119. doi: 10.3390/ijms21093119

586

587

58826 - Lander GC, Baudoux AC, Azam F, Potter CS, Carragher B, Johnson JE. Capsomer  
589dynamics and stabilization in the T = 12 marine bacteriophage SIO-2 and its procapsid  
590studied by CryoEM. *Structure.* 2012;20(3):498–503. doi:10.1016/j.str.2012.01.007

591

59227 - Huiskonen J, Kivelä H, Bamford D, et al. The PM2 virion has a novel organization with  
593an internal membrane and pentameric receptor binding spikes. *Nat Struct Mol Biol*  
5942004;11:850–856. <https://doi.org/10.1038/nsmb807>

595

59628 - Laanto E, Mäntynen S, De Colibus L, et al. Virus found in a boreal lake links ssDNA and  
597dsDNA viruses. *Proc Natl Acad Sci U S A*. 2017;114(31):8378–8383.  
598doi:10.1073/pnas.1703834114

599

60029 - Rissanen I, Grimes JM, Pawlowski A et al. Bacteriophage P23-77 Capsid Protein  
601Structures Reveal the Archetype of an Ancient Branch from a Major Virus Lineage *Structure*.  
6022013; 21(5): 718–726. doi: 10.1016/j.str.2013.02.026

603

604

605

606

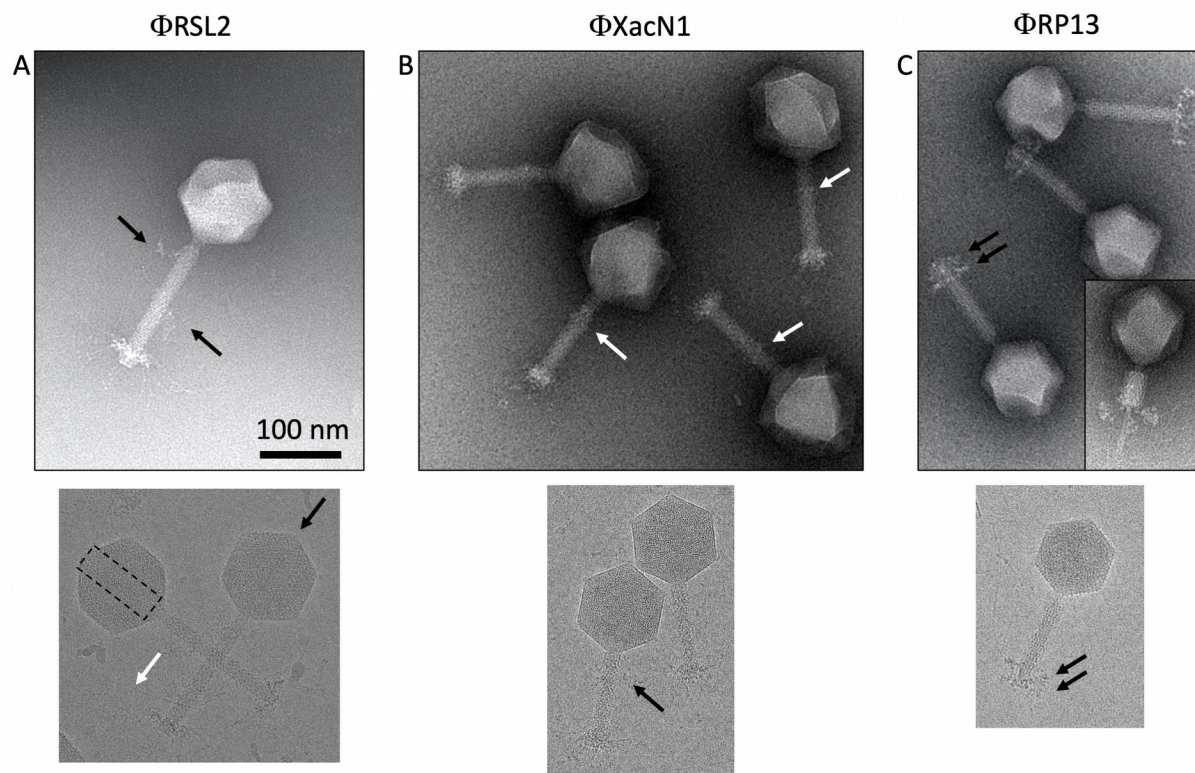


Figure 1, Neumann et al.

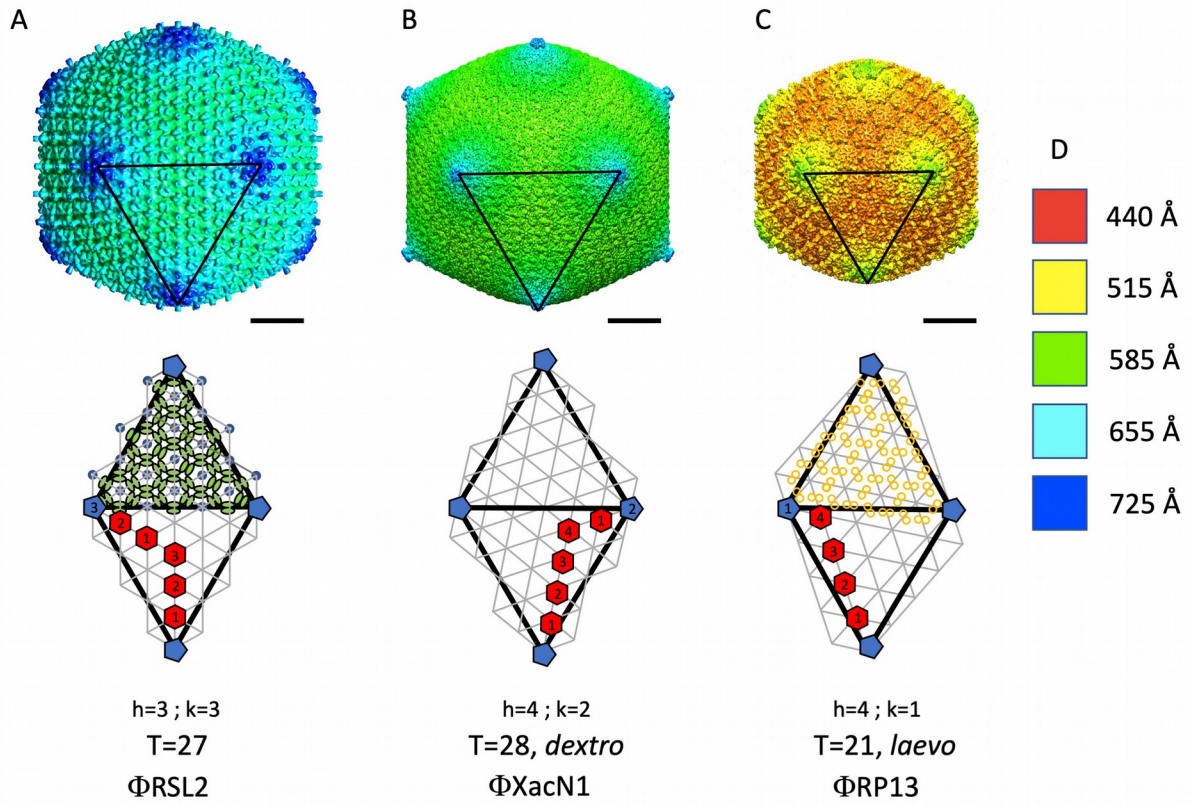


Figure 2 Neumann et al.

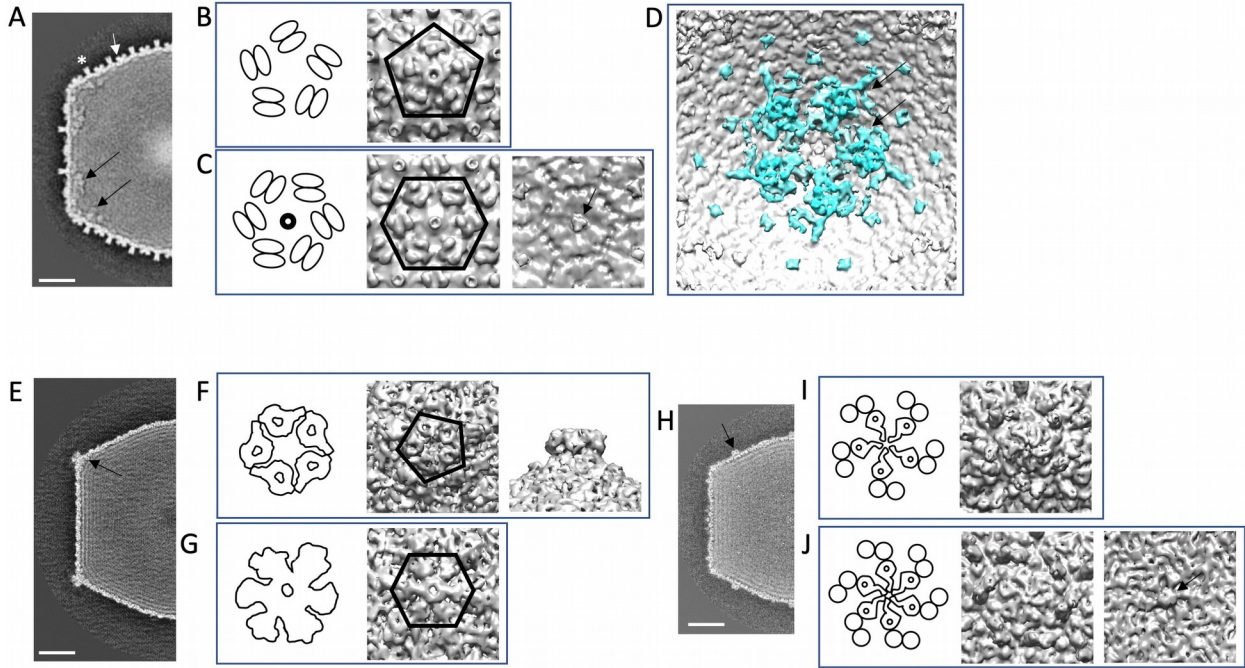
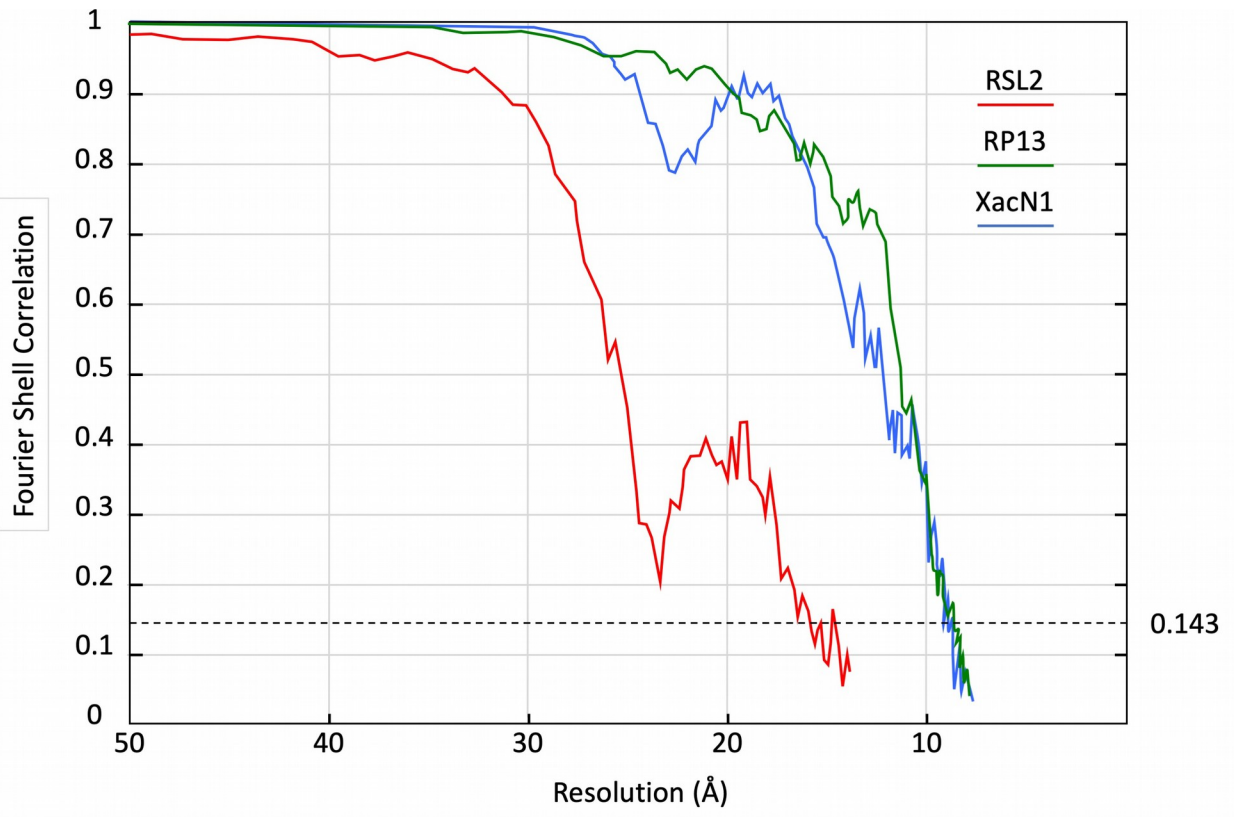
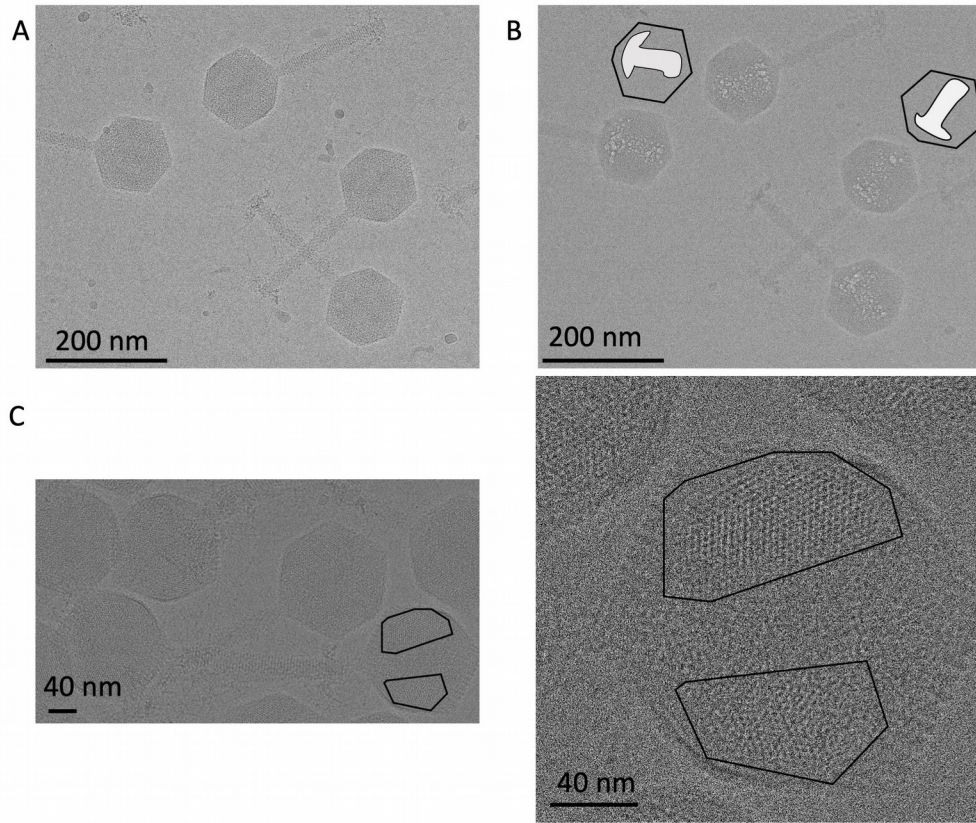


Figure 3 Neumann et al.

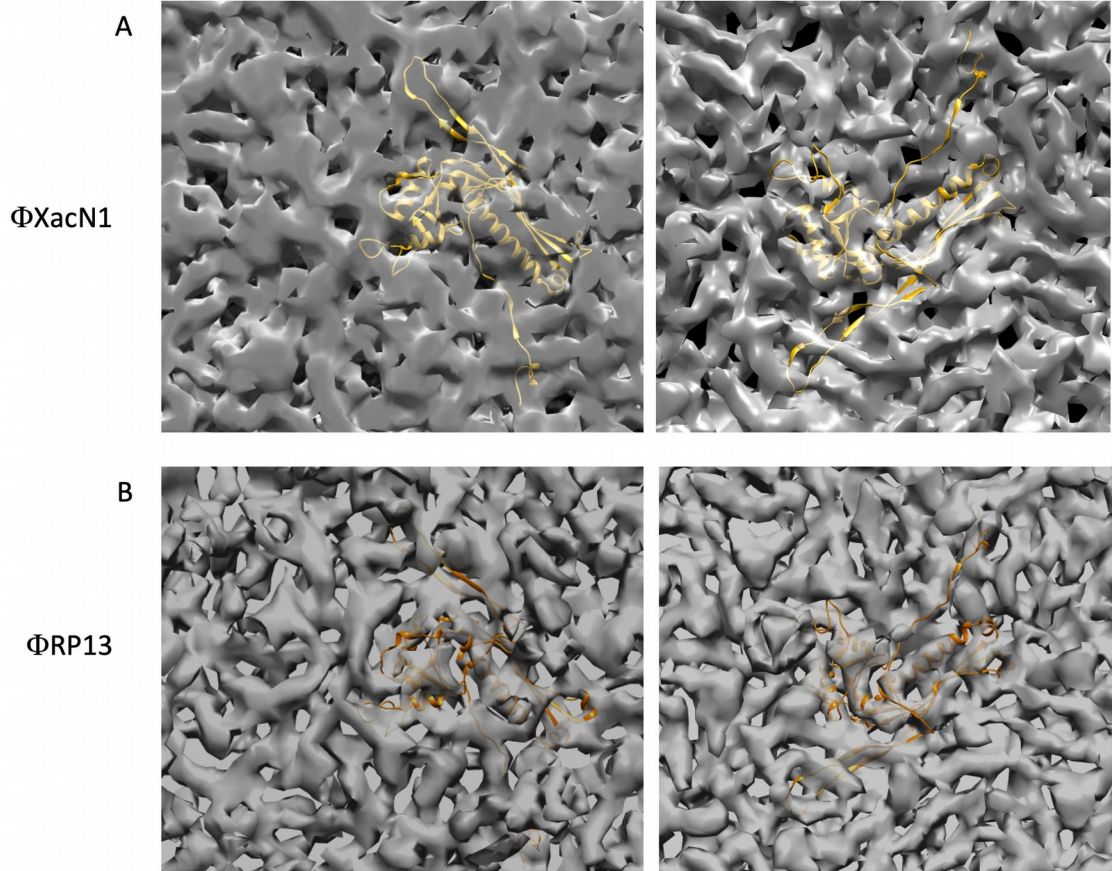




Supplemental Figure 1 Neumann et al.



Supplemental Figure 2 Neumann et al.



Supplemental Figure 3 Neumann et al.

<b>Data collection and processing</b>	<b>RSL2</b>	<b>XacN1</b>	<b>RP13</b>
Magnification	12,000	20,000	20,000
Voltage (kV)	300	300	300
Electron exposure (e-/ Å <sup>2</sup> )	40	40	40
Pixel size (after binning)	6.57 Å	3.88 Å	3.88 Å
Defocus range (µm)	-1.3 to -4.5	-1.0 to -3.5	-1.5 to -4.0
Symmetry imposed	532	532	532
Number of micrographs	73	889	659
Initial number of selected particles	499	1775	1311
Number of particles for the final reconstruction	250	1149	669
Map resolution (Å)	16	9.1	9.5
FSC threshold	0.143	0.143	0.143
Applied B-Factor (Å <sup>2</sup> )	None	-671	-716

Table 1 Neumann et al.

	$\Phi$ RSL2	$\Phi$ XacN1	$\Phi$ RP13
<b>Capsid</b>			
<b>Capsid diameter</b> 2-fold axis	128 nm	115 nm	97 nm
<b>Capsid diameter</b> vertex to vertex	139 nm	134 nm	114 nm
<b>Internal diameter of the capsid</b> 2-fold axis	<b>108 nm</b>	<b>108 nm</b>	<b>89,5 nm</b>
<b>Capsid volume (x</b> <b>10<sup>3</sup> nm<sup>3</sup>)</b>	<b>830</b>	<b>790</b>	<b>460</b>
<b>Capsid thickness</b>	<b>42 Å</b>	<b>38 Å</b>	<b>40 Å</b>
<b>T Number; h; k</b>	<b>T=27 h=3, k=3</b>	<b>T=28,d h=4, k=2</b>	<b>T=21,l h=4, k=1</b>
<b>Decoration protein</b> <b>Number of dimers</b>	<b>810</b>	<b>0</b>	<b>630</b>
<b>Decoration proteins</b> <b>Number of spikes</b> <b>(6-fold)</b>	<b>260</b>	<b>0</b>	<b>0</b>
<b>Tail</b>			
<b>Tail</b>			
<b>Length</b>	<b>1650 Å</b>	<b>1180 Å</b>	<b>1010 Å</b>
<b>Number of repeats</b>	<b>44</b>	<b>31</b>	<b>28</b>
<b>Pitch</b>	<b>37.5 Å</b>	<b>38 Å</b>	<b>36 Å</b>
<b>DNA</b>			
<b>DNA (kbp)</b>	<b>224 kbp</b>	<b>385 kbp</b>	<b>180 kbp</b>
<b>DNA spacing</b>		<b>23.6 Å</b>	<b>26.3 Å</b>
<b>Avg density of packaged DNA (bp/nm<sup>3</sup>)</b>	<b>0.29</b>	<b>0.49</b>	<b>0.39</b>

**Table 2 Neumann et al.**